Observation of $^1D - ^1S$ forbidden optical emission of atomic oxygen in atmospheric-pressure N_2/O_2 plasma jet

Koichi Sasaki[*], **Shusuke Nishiyama**[**], and **Naoki Shirai**

Division of Applied Quantum Science and Engineering, Hokkaido University, Kita 13, Nishi 8, Kita-ku, Sapporo 060-8628, Japan

Key words $^1D - ^1S$ forbidden transition, atomic oxygen, ON_2^* excimer, atmospheric-pressure plasma jet

We observed green optical emission from an atmospheric-pressure N_2/O_2 plasma jet. The green optical emission was composed of a line emission at $\lambda = 557.71 \pm 0.03$ nm and a broadband component at $530 \leq \lambda \leq 560$ nm. The line emission was assigned to the $^1D - ^1S$ forbidden transition of atomic oxygen, whereas the broadband emission was due to the formation of $O(^1S)N_2$ excimer. We measured the absolute densities of $O(^1S)$ and $O(^1S)N_2$ using a spectrograph with the absolute sensitivity calibration, and we discussed the kinetics in the green plasma jet on the basis of the absolute $O(^1S)$ and $O(^1S)N_2$ densities. According to the rate coefficients and the transition probabilities reported in literature, the present experimental results are explained if the densities of $N_2(A^3\Sigma_u^+)$ and $O(^3P)$ are 9×10^{13} and 3×10^{13} cm^{-3}, respectively.

1 Introduction

It is well known that the green light from auroras is due to the $^1D - ^1S$ forbidden transition of atomic oxygen at a wavelength of 557.73 nm. The transition probability of this line is just 1.26 s^{-1} [1]. Because of the small transition probability, this forbidden transition is rarely observed in laboratory plasmas. In particular, in low-pressure, low-temperature oxygen-containing plasmas, which are widely used in industrial material processing, the intensity of this forbidden line does not exceed the noise level in the optical emission spectrum, except the very recent work by Fiebrandt and coworkers [2].

Recently, atmospheric-pressure plasmas attract much attention of many researchers since they have potential applications in medicine [3–5], agriculture [6–8], and water treatment [9,10]. Since optical emission spectroscopy is a simple method to identify active chemical species in plasmas, various optical emission spectra are displayed in many papers which report the characterization of atmospheric-pressure plasmas. The authors of some papers

[*] Corresponding author: e-mail: sasaki@qe.eng.hokudai.ac.jp, Phone: +81 11 706 6654, Fax: +81 11 706 6655

[**] Present address: Japan Health Care College

notice the optical emission at around 557 nm in oxygen containing atmospheric-pressure plasmas [11–17]. The shapes of the optical emission spectra are not narrow lines but have molecular-band structures. They assigned the band emission to the formation of OAr^* [15] and ON_2^* excimers [12–14, 17]. The intensity of the excimer optical emission is usually lower than the intensity of the first positive system of molecular nitrogen [13, 14]. However, Motomura *et al.* [15] and Lee *et al.* [17] observed dominant optical emissions of OAr^* and ON_2^* excimers, respectively, and in these cases green plasmas are seen by naked eyes. Although the observations of the green laboratory plasmas are impressive, unfortunately, the wavelength resolutions of the spectra shown in the papers are not fine, and we cannot see the detailed spectrum of the green optical emission from the atmospheric-pressure plasmas.

We are working on the development of an atmospheric-pressure plasma jet which can be operated using nitrogen as the working gas with the intention of applying it to the suppression of potato sprout [18]. In the series of experiments using the nitrogen plasma jet, we noticed that the plasma emitted green optical emission when we admixed a small amount of oxygen. In this paper, we report fine-resolution optical emission spectra of the ${}^1D - {}^1S$ forbidden transition with the enhancement by the formation of the ON_2^* excimer. We discussed the kinetics in the plasma jet on the basis of the absolute densities of $O({}^1S)$ and $O({}^1S)N_2$.

2 Experiment

Figure 1(a) shows the schematic illustration of the plasma jet source we used in the experiment. A quartz tube with an inner diameter of 4 mm was used for the discharge tube, and it was surrounded by an copper electrode with a length of 20 mm. A tungsten rod electrode was positioned at the center of the discharge tube. The tungsten electrode was not covered with dielectrics. Nitrogen was fed from the bottom of the quartz tube at a flow rate of 7 slm, and oxygen was admixed into nitrogen at a flow rate less than 100 sccm. The copper electrode was electrically grounded, and the tungsten rod electrode was connected to a bipolar pulsed power supply. The waveforms of the discharge voltage and the discharge current are shown in Fig. 1(b). The discharge voltage was approximately 25 kV (peak-to-peak), while the discharge current, which was measured by inserting a register between the copper electrode and the electrical ground, was several amperes. This means extremely high instantaneous power during the pulsed discharge. The durations of the positive and negative high voltages were approximately 3 μs, and the repetition frequency of the high-voltage pulse was 10 kHz.

The optical emission from the plasma jet was projected onto the entrance side of optical fibers using a lens from the radial direction, and the optical fibers guided the optical emission to spectrographs. The distance between the end of the quartz tube and the measurement position was 5 mm. We used two spectrographs in the present experiment. One was a small spectrograph which had a low wavelength resolution and a wide measurement range (Ocean Optics, USB2000). The other was a Czerny-Turner spectrograph with a focal length of 50 cm (Acton, 2500i). The groove densities of the diffraction gratings we used in the latter spectrograph were 600 and 2400 g/mm. The latter spectrograph was equipped with a charge-coupled device camera with a gated image

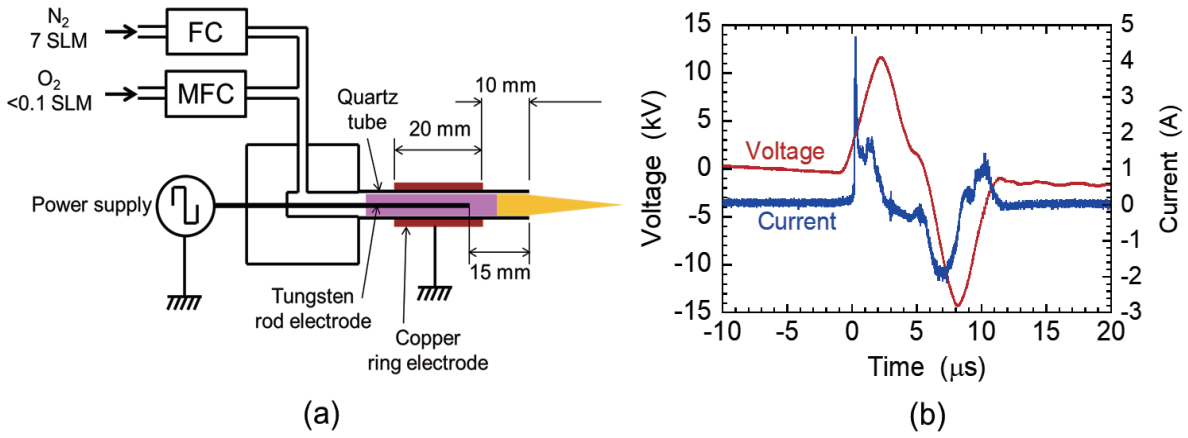

Fig. 1 (a) Schematic of the plasma jet source and (b) the waveforms of the discharge voltage and the discharge current.

intensifier (ICCD camera). The absolute sensitivity of the spectrograph including the ICCD camera and the lens was calibrated using a tungsten standard lamp, so that we obtained the number of photons emitted from the plasma jet per unit volume and unit time. We evaluated the absolute densities of the excited states from the number of photons with the help of the knowledge on the transition probabilities.

3 Results

The photographs of the plasma jets, which were taken using a consumer-class digital camera, are shown in Fig. 2. Figure 2(a) is the photograph of the nitrogen discharge. The color of the discharge in the electrode region was pink, which is the usual color of nitrogen discharges. On the other hand, the color of the jet part was orange as shown in Fig. 2(a). When we added oxygen at a flow rate of 50 sccm into nitrogen, we observed the green optical emission from the plasma jet as shown in Fig. 2(b). We examined the temporal variations of the optical emission intensities from the plasma jets. As a result, we observed steady-state optical emission intensities, even through the discharge power was intermittent at a frequency of 10 kHz.

The spectra of the orange and green plasma jets are shown in Figs. 3(a) and 3(b), respectively. These spectra were measured using the small spectrograph with a low resolution of 2 nm. The sensitivity as a function of the wavelength was not calibrated in these spectra. As shown in Fig. 3(a), the optical emission from the pure nitrogen plasma jet (Fig. 2(a)) was composed of the first and second positive systems of molecular nitrogen. The spectrum of the second positive system in the UV region is similar to those observed in many nitrogen plasmas. A remarkable feature of the spectrum shown in Fig. 3(a) is seen in the first positive system, where we observed the dominant optical emission around 580 nm. This optical emission is the source of the orange plasma jet shown in Fig. 2(a), and is assigned to the $\Delta v = 4$ transitions from $\mathrm{N}_2(B^3\Pi_g, 10 \leq v \leq 12)$. When we added a small amount (50 sccm or 0.7% of nitrogen) of oxygen into the nitrogen discharge, we observed the disappearance of

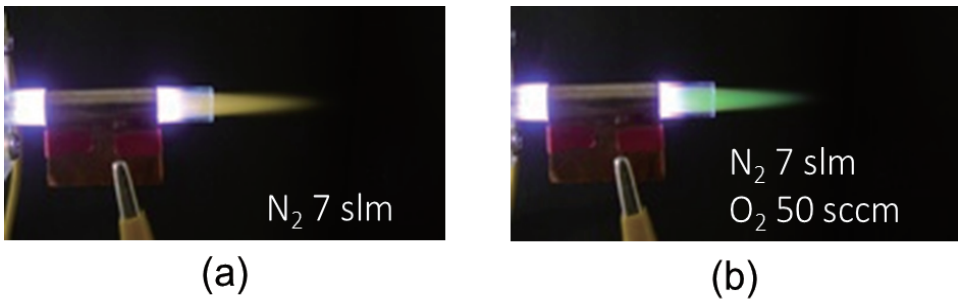

Fig. 2 Photographs of the plasma jets with (a) pure nitrogen and (b) mixture of nitrogen and oxygen (50 sccm).

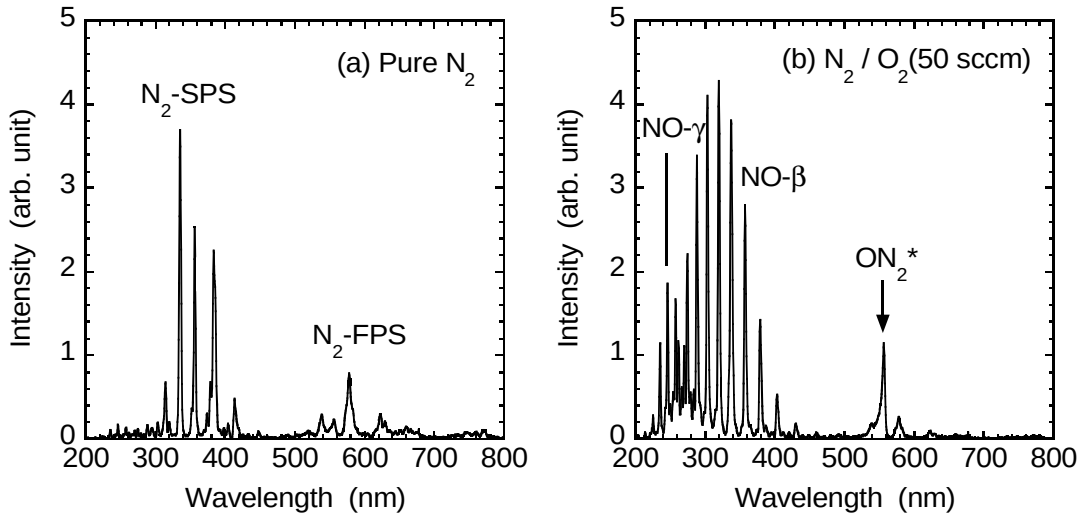

Fig. 3 Low-resolution spectra of the plasma jets with (a) pure nitrogen and (b) mixture of nitrogen and oxygen (50 sccm).

the optical emissions of the first and second positive systems of molecular nitrogen, as shown in Fig. 3(b), except the optical emission around 580 nm. The optical emission in the UV region was assigned to the β and γ bands of nitrogen monoxide. Another remarkable point in the spectrum shown in Fig. 3(b) is the appearance of the broad spectrum at $530 \leq \lambda \leq 560$ nm. The spectral shape is similar to those shown in literature [12, 14–17]. This optical emission is the source of the green plasma jet shown in Fig. 2(b).

Figure 4(a) shows the medium-resolution spectra of the N_2 and N_2/O_2 plasma jets, which were measured using the Czerny-Turner spectrograph with a focal length of 50 cm. The flow rate of oxygen in the N_2/O_2 plasma jet was 48 sccm. The groove density of the diffraction grating was 600 g/mm, and the width of the entrance slit was 10 μm. The wavelength resolution was 0.2 nm. These spectra include the dark level of the spectrograph. The spectra observed at $535 \leq \lambda \leq 545$ nm are assigned to the $\Delta v = 5$ transitions from $N_2(B^3\Pi_g, 10 \leq v \leq 12)$ (the first positive system). The appearance of the smooth broad spectrum is caused by the oxygen admixture. The weak broad spectrum in the nitrogen discharge at the same wavelength range may be due to impurity oxygen. To

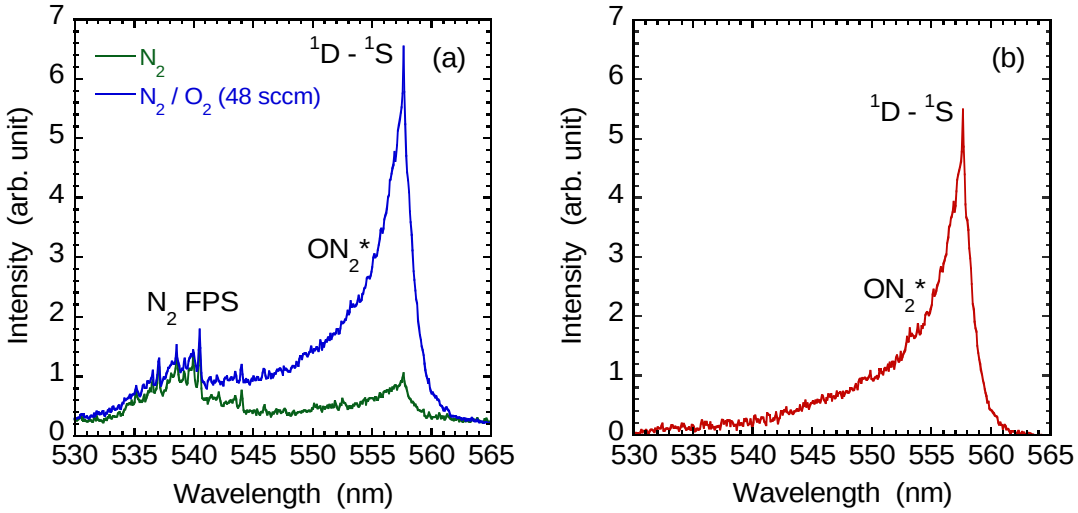

Fig. 4 (a) Medium-resolution spectra of the N_2 and N_2/O_2 (48 sccm) plasma jets. (b) is the difference spectra between the two curves shown in (a).

eliminate the dark level and the optical emission of molecular nitrogen, we calculated the difference between the two spectra shown in Fig. 4(a). Figure 4(b) is the difference spectrum, which shows the influence of the oxygen admixture to the nitrogen plasma jet. The broadband optical emission spreads over the wavelength range between 530 and 560 nm, as shown in Fig. 4(b). The spectrum shown in Fig. 4(b) has a smooth curve at $530 \leq \lambda \leq 545$ nm, suggesting that the optical emission intensities of the $\Delta v = 5$ transitions from $N_2(B^3\Pi_g, 10 \leq v \leq 12)$ (the first positive system) was not affected considerably by the admixture of oxygen at a flow rate of 48 sccm. The optical emission intensities due to the transitions from $N_2(B^3\Pi_g, 10 \leq v \leq 12)$ were sensitive to the amount of the oxygen admixture, and they became weaker when the flow rate of oxygen was 50 sccm, as shown in Fig. 3.

Figure 5 was observed at the same experimental conditions as those in Fig. 4 except that we employed the diffraction grating with the groove density of 2400 g/mm. The wavelength resolution was 0.05 nm. The wavelength axis in Fig. 5 was calibrated by the following procedure. First, we operated a tunable optical parametric oscillator (OPO). The wavelength of the OPO laser light was adjusted at 557.73 nm using a wave meter with an accuracy of ± 5 pm. Second, we measured the spectrum of the OPO laser light using the same spectrograph as that used in Fig. 5, and we identified the difference between the true and apparent wavelengths in the spectrograph. The fine-resolution spectra shown in Fig. 5 indicate that the spectra shown in Fig. 4 include a sharp line component. The wavelength of the line emission was 557.71 ± 0.03 nm. The weak line emission observed in the nitrogen plasma jet at the same wavelength may be attributable to impurity oxygen.

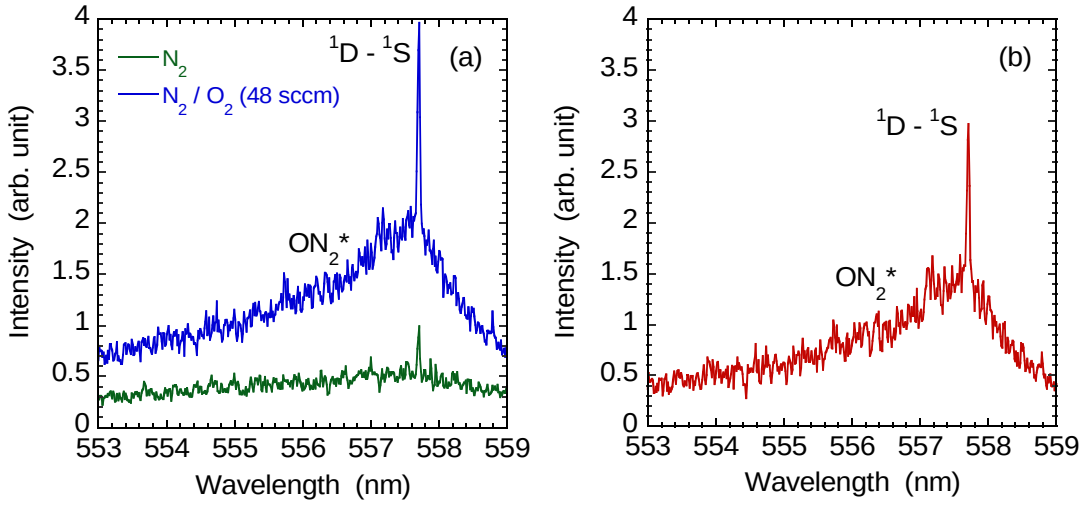

Fig. 5 (a) Fine-resolution spectra of the N_2 and N_2/O_2 (48 sccm) plasma jets. (b) is the difference spectra between the two curves shown in (a).

4 Discussion

The kinetics of electronic excited states in atmospheric-pressure N_2/O_2 spatial afterglow have been investigated by Pointu and coworkers [13]. According to them, the remarkable optical emission spectra of the first positive system of molecular nitrogen around 580 and 540 nm, which are shown in Figs. 3 and 4(a), respectively, are understood to be due to the production of $N_2(B^3\Pi_g, v = 11)$ by $N + N + N_2 \rightarrow N_2(B^3\Pi_g, v = 11) + N_2$. The shift from the second positive system of molecular nitrogen to the β and γ bands of nitrogen monoxide is partly attributed to $O + N_2 \rightarrow NO + N$ and $N + O_2 \rightarrow NO + O$. It is known that vibrational excited states of molecular nitrogen at the electronic ground state play important roles in the former reaction [19]. In addition, $N + O + N_2 \rightarrow NO(B^2\Pi) + N_2$ and $N_2(A^3\Sigma_u^+) + NO \rightarrow NO(A^2\Sigma^+) + N_2$ contribute to the β and γ bands of nitrogen monoxide, respectively [13].

The wavelength of the line emission shown in Fig. 5 is exactly equal to the wavelength of the $^1D - ^1S$ forbidden transition of atomic oxygen at 557.734 nm. The transition probability of this forbidden line is just $A_a = 1.26\ s^{-1}$ [1]. The absolute density of $O(^1S)$ is evaluated using the following equation,

$$[O(^1S)] = \frac{S_P}{S_L}\frac{I_L 4\pi\Delta\lambda_L}{h\nu A_a D}\frac{G_L\Delta T_L}{G_P\Delta T_P}, \quad (1)$$

where S_P and S_L are the signals from the spectrograph when detecting the optical emissions from the plasma and the tungsten standard lamp, respectively, I_L is the intensity of the lamp emission which is given in the unit of $Wcm^{-3}sr^{-1}$, $h\nu$ is the photon energy, D is the diameter of the plasma jet, $\Delta\lambda_L$ is the resolution of the spectrograph when measuring S_L, G_P and G_L are the gains of the ICCD camera when measuring S_P and S_L, respectively, and ΔT_P and ΔT_L are the gate widths when measuring S_P and S_L, respectively. From the spectrum shown in Fig. 5(a) (the blue spectrum), we obtained $[O(^1S)] = 1.6 \times 10^{12}\ cm^{-3}$.

It is known that the broad optical emission at $530 \leq \lambda \leq 560$ nm is due to the formation of $O(^1S)N_2$ excimer [20–22]. The excimer is unstable, and it decays spontaneously by emitting a photon ($O(^1S)N_2 \rightarrow O(^1D) + N_2 + h\nu$). The transition probability is $A_m = 1 \times 10^7$ s^{-1} [14, 16]. The absolute density of $O(^1S)N_2$ is evaluated by the same manner as that for the evaluation of $[O(^1S)]$ with small modification considering the broadband spectrum,

$$[O(^1S)N_2] = \frac{4\pi}{A_m D} \frac{G_L \Delta T_L}{G_P \Delta T_P} \int \frac{S_P(\lambda)}{S_L(\lambda)} \frac{I_L(\lambda)}{h\nu} d\lambda. \quad (2)$$

We obtained $[O(^1S)N_2] = 2.5 \times 10^7$ cm^{-3} from the spectrum shown in Fig. 4(a). Although the subtraction of the first positive system of molecular nitrogen from the overlapped spectrum may cause the ambiguity in the evaluation of the $O(^1S)N_2$ density, the error is less than 10% since the first positive system overlaps with the tail part of the spectrum of the excimer emission.

The production process of $O(^1S)N_2$ is the forward reaction of

$$O(^1S) + N_2 + N_2 \leftrightarrow O(^1S)N_2 + N_2. \quad (3)$$

The rate coefficients of the forward and reverse reactions are $k_+ = 2 \times 10^{-36}$ cm^6/s [14, 16] and $k_- = 5 \times 10^{-12}$ cm^3/s [16], respectively. If we limit the loss processes of $O(^1S)N_2$ to the spontaneous emission and the reverse reaction of (3), the rate equation for $[O(^1S)N_2]$ is given by

$$\frac{d[O(^1S)N_2]}{dt} = k_+[O(^1S)][N_2]^2 - k_-[O(^1S)N_2][N_2] - A_m[O(^1S)N_2]. \quad (4)$$

From this equation, we obtain $[O(^1S)N_2]/[O(^1S)] \simeq 6 \times 10^{-6}$ at the steady state, which agrees with the experimental result within a factor of 3. On the other hand, the rate equation for $[O(^1S)]$ is given by

$$\frac{d[O(^1S)]}{dt} = P - k_+[O(^1S)][N_2]^2 + k_-[O(^1S)N_2][N_2] - \nu_q[O(^1S)] - A_a[O(^1S)], \quad (5)$$

where P and ν_q are the production rate and the frequency of collisional quenching of $O(^1S)$, respectively. The frequency of collisional quenching is evaluated by $\nu_q = k_q^{N2}[N_2] + k_q^{O2}[O_2]$ with $k_q^{N2} = 5 \times 10^{-17}$ and $k_q^{O2} = 2.8 \times 10^{-13}$ cm^3/s being the rate coefficients of collisional quenching by N_2 and O_2, respectively [23]. Considering the values of k_+, k_-, k_q^{N2}, k_q^{O2}, A_a, $[O(^1S)]$, and $[O(^1S)N_2]$, it is understood that $\nu_q[O(^1S)]$ dominates the right hand side of eq. (5) in the present experimental condition, and we obtain $P \simeq 5.7 \times 10^{16}$ cm^{-3}s^{-1} for the production rate of $O(^1S)$.

It is supposed that the plasma jets shown in Fig. 2 are not active discharge plasmas but are spatial afterglows, since the propagation of the ionization wave is not efficient in nitrogen [24]. This speculation is supported by the fact that the plasma jets have different colors (or optical emission spectra) from the active discharges in the electrode region. In addition, the steady-state optical emission intensity in spite of the intermittent discharge at 10 kHz suggests that the plasma jet is sustained by long-lived species. Many theoretical and experimental investigations have reported the spatial afterglow phenomena in nitrogen discharges [25–27]. It has been shown

that the spatial afterglow is sustained by the transport of long-lived vibrational excited states of molecular nitrogen. The metastable $A^3\Sigma_u^+$ state is produced by the collision between $N_2(X^1\Sigma_g^+, v)$ and atomic nitrogen. The radiative electronic excited states ($B^3\Pi_g$ and $C^3\Pi_u$) are produced by collision between two $N_2(A^3\Sigma_u^+)$ and by collision between $N_2(A^3\Sigma_u^+)$ and $N_2(X^1\Sigma_g^+, v)$. These electronic excited states are not produced by electron impact excitation. In this situation, electron impact excitation does not contribute to the production of $O(^1S)$, and the dominant production process of $O(^1S)$ is considered to be

$$O(^3P) + N_2(A^3\Sigma_u^+) \rightarrow O(^1S) + N_2. \tag{6}$$

The rate coefficient of this reaction is $k_p = 2.1 \times 10^{-11}$ cm^3/s [14].

We measured the density of $O(^3P)$ (the ground state) by two-photon absorption laser-induced fluorescence (TALIF). It employed the conventional excitation scheme from the $2p^4\,^3P$ to $3p^3P$ states using a pulsed dye laser at 225.58 nm, and the fluorescence by the transition from the $3p^3P$ to $3s^3S$ states (844.64 nm) was detected using an ICCD camera. The laser energy was attenuated to the level where the TALIF intensity caused by the photodissociation of molecular oxygen was negligible. The absolute $O(^3P)$ density was evaluated by comparing the TALIF intensity observed in the plasma jet with that observed by the photodissociation of molecular oxygen at a known pressure [28]. The absolute $O(^3P)$ density was approximately $[O(^3P)] = 3 \times 10^{13}$ cm^{-3}. Therefore, $[N_2(A^3\Sigma_u^+)] = P/(k_p[O(^3P)]) = 9 \times 10^{13}$ cm^{-3} is necessary for the density of $N_2(A^3\Sigma_u^+)$ to sustain the spatial afterglow with the remarkable green optical emission shown in Fig. 2(b). We believe it is possible, since $[N_2(A^3\Sigma_u^+)] = 9 \times 10^{13}$ cm^{-3} is just 5 ppm of the ground-state molecular nitrogen. The $N_2(A^3\Sigma_u^+)$ densities in atmospheric-pressure discharges, which are reported in literature, range between 1×10^{13} and 5×10^{14} cm^{-3} [29–33]. We also measured the density of atomic nitrogen by TALIF for the reference. The excitation scheme was from the $2p^3\,^4S$ to $3p^4S$ states using the pulsed dye laser at 206.65 nm, and the fluorescence by the transition from the $3p^4S$ to $3s^4P$ states (742-746 nm) was detected using the ICCD camera. The absolute density was evaluated by comparting the TALIF intensity of nitrogen with that of krypton at a known pressure [34]. The absolute density of $N(^4S)$ was approximately $[N(^4S)] = 3 \times 10^{15}$ cm^{-3} in the same plasma jet.

5 Conclusions

In this work, we observed the clear optical emission due to the $^1D - ^1S$ forbidden transition of atomic oxygen in the atmospheric-pressure N_2/O_2 (0.7%) plasma jet. The green laboratory plasma with the auroral optical emission is impressive and is appears to be surprising. However, according to the rate coefficients and the transition probabilities reported in literature, it is possible to observe the green plasma jet if the densities of $N_2(A^3\Sigma_u^+)$ and $O(^3P)$ are 9×10^{13} and 3×10^{13} cm^{-3}, respectively. $N_2(A^3\Sigma_u^+)$ is produced by the transport of vibrational excited states of molecular nitrogen in the present experimental condition.

Acknowledgements The authors are grateful to K. Ueno and M. Shimabayashi for the measurements of $O(^3P)$ and $N(^4S)$ densities by TALIF.

References

[1] *NIST Atomic Spectra Databese*, https://www.nist.gov/pml/atomic-spectra-database.

[2] M. Fiebrandt, N. Bibinov, and P. Awakowicz, *Plasma Sources Sci. Technol.* **2020**, 29, 045018.

[3] G. Fridman, G. Friedman, A. Gutsol, A. B. Shekhter, V. N. Vasilets, and A. Fridman, *Plasma Process. Polym.* **2008**, 5, 503.

[4] M. G. Kong, G. Kroesen, G. Morfill, T. Nosenko, T. Shimizu, J. van Dijk, and J. L. Zimmermann, *New J. Phys.* **2009**, 11, 115012.

[5] K. -D. Weltmann, M. Polak, K. Masur, T. von Woedtke, J. Winter, and S. Reuter, *Contrib. Plasma Phys.* **2012**, 52, 644.

[6] S. Perni, D. W. Liu, G. Shama, and M. G. Kong, *J. Food Prot.* **2008**, 71, 302.

[7] M. Ito, J.-S. Oh, T. Ohta, M. Shiratani, and M. Hori, *Plasma Process Polym.* **2017**, e1700073.

[8] R. Thirumdasa, A. Kothakotab, U. Annapurec, K. Siliverud, R. Blundelle, R. Gattf, and V. P. Valdramidisg, *Trends Food Sci. Technol.* **2018**, 77, 21.

[9] T. Miichi, N. Hayashi, S. Ihara, S. Satoh, and C. Yamabe, *Ozone Sci. Eng.* **2002**, 24, 471.

[10] B. R. Locke, M. Sato, P. Sunka, M. R. Hoffmann, and J.-S. Chang, *Ind. Eng. Chem. Res.* **2006**, 45, 882.

[11] I. P. Vinogradov and K. Wiesemann, *Plasma Sources Sci. Technol.* **1997**, 6, 307.

[12] K. V. Kozlov, R. Brandenburg, H.-E. Wagner, A. M. Morozov, and P. Michel, *J. Phys. D: Appl. Phys.* **2005**, 38, 518.

[13] A.-M. Pointu, A. Ricard, B. Dodet, E. Odic, J. Larbre, and M. Ganciu, *J. Phys. D: Appl. Phys.* **2005**, 38, 1905.

[14] R. Brandenburg, V. A. Maiorov, Yu B. Golubovskii, H.-E. Wagner, J. Behnke, and J. F. Behnke, *J. Phys. D: Appl. Phys.* **2005**, 38, 2187.

[15] H. Motomura, H. Matsuba, M. Kawata, and M. Jinno, *Jpn. J. Appl. Phys.* **2007**, 46, L939.

[16] E. Panousis, A. Ricard, J.-F. Loiseau, F. Clément, and B. Held, *J. Phys. D: Appl. Phys.* **2009**, 42, 205201.

[17] H. V. Lee Jr., L. . D. Rosario, R. B. Tumlos, H. J. Ramos, L. M. T. Bo-ot, and M. N. Soriano, *Jpn. J. Appl. Phys.* **2018**, 57, 066102.

[18] K. Ueno, S. Nishiyama, and K. Sasaki, *Proceedings of Joint Conference of XXXIV International Conference on Phenomena in Ionized Gases and the 10th International Conference on Reactive Plasmas* **2019**, PO15PM-031.

[19] W. Wang, B. Patil, S. Heijkers, V. Hessel, and A. Bogaerts, *ChemSusChem* **2017**, 10, 2145.

[20] R. F. Hampson Jr and H. Okabe, *J. Chem. Phys.* **1970**, 52, 1930.

[21] D. L. Cunningham and K. C. Clark, *J. Chem. Phys.* **1974**, 61, 1118.

[22] G. Black, R. l. Sharpless, and T. G. Sianger, *J. Chem. Phys.* **1975**, 63, 4546.

[23] F. Tochikubo and T. H. Teich, *Jpn. J. Appl. Phys.* **2000**, 39, 1343.

[24] X. Lu, G. V. Naidis, M. Laroussi, and K. Ostrikov, *Phys. Rep.* **2014**, 540 123.

[25] N. Sadeghi, C. Foissac, and P. Supiot, *J. Phys. D: Appl. Phys.* **2001**, 34, 1779.

[26] P. A. Sá, V. Guerra, J. Loureiro, and N Sadeghi, *J. Phys. D: Appl. Phys.* **2004**, 37, 221.

[27] V. Guerra, P. A. Sá, and J. Loureiro, *Eur. Phys. J. Appl. Phys.* **2004**, 28, 125.

[28] K. Kadota, Y. Konno, K. Aoto, T. Shoji, and T. Sato, *Jpn. J. Appl. Phys.* **1994**, 33, 4308.

[29] Y. Teramoto, R. Ono, and T. Oda, *J. Phys. D: Appl. Phys.* **2009**, 42, 235205.

[30] S. Nemschokmichal and J. Meichsner, *Plasma Sources Sci. Technol.* **2013**, 22, 015005.

[31] M. Šimek, P. F. Ambrico, and V. Prukner, *J. Phys. D: Appl. Phys.* **2015**, 48, 265202.

[32] E. R. Jans, K. Frederickson, T. A. Miller, and I. V. Adamovich, *J. Mol. Spectrosc.* **2015**, 365, 111205.

[33] S. Kanazawa, A. Ohno, T. Furuki, K. Tachibana, R. Ichiki, A. Suzuki, K. Kuroi, K. Suzumura, T. Tanaka, K. Motegi, M. Kocik, and J. Mizeraczyk, *J. Electrostat.* **2020**, 103, 103419.

[34] K. Niemi, V. Schulz-von der Gathen, and H. F. Dëbele, *J. Phys. D: Appl. Phys.* **2001**, 34, 2330.